

Effect of Temperature on Detonation Propagation in Composition B

John D. Yeager*, Scott I. Jackson*, Mark Short*

*Shock and Detonation Physics
Los Alamos National Laboratory, Los Alamos, New Mexico, USA

Abstract. Composition B is a melt-castable explosive consisting of RDX crystals in a TNT matrix. At elevated temperatures, the TNT can flow or even melt, which affects the particle distribution and therefore the detonation propagation. To study this phenomenon, rate stick experiments were conducted at ambient conditions, at temperatures below the TNT melt, and at temperatures above the TNT melt. We fielded shorting pins to measure the detonation velocity and a streak camera to record the detonation breakout. We report the measured velocities as a function of temperature and discuss the effect of temperature on detonation propagation. The need for temperature-dependent Composition B data in detonation shock dynamics simulations is discussed.

Introduction

Composition B is a melt-castable explosive containing approximately 60 wt% cyclotrimethylene trinitramine (RDX) in a trinitrotoluene (TNT) matrix. Various formulations of Composition B may also include up to 1% wax. Figure 1 shows scanning electron micrographs of the Composition B with and without preferential etching of the TNT. During heating or melt-casting, the RDX particles can settle as the TNT becomes molten and starts to flow. TNT melts at 80°C but Composition B transitions from stable solid to a slurry at 79°C.¹ This thermal instability can result in anisotropic detonation properties as the RDX particles become unevenly distributed. This is expected to affect shock response and initiation and growth within the material, which in general is being studied elsewhere.^{2, 3} However, the RDX distribution effect is convolved with the difference in properties between solid and molten TNT.

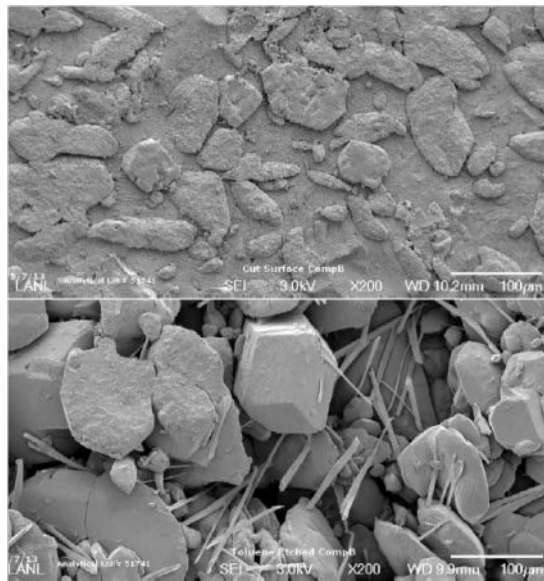


Fig. 1. Cut surface of Composition B-3 (top) and etched surface (bottom). Large crystals are RDX, while the needle-like crystals are TNT.

These competing effects cause difficulties in both experimental and theoretical interpretation of elevated temperature behavior of Composition B.

Experimentally, solid-solid phase transitions in high explosive (HE) and plastic-bonded explosive (PBX) systems can affect density and crystal structure, while solid-liquid transitions additionally affect part stability (i.e. altering the experimental geometry), vapor pressure, and chemical reaction rate.⁴⁻⁸ Corresponding effects on shock and detonation properties are either known or implied.⁸⁻¹⁰ Theoretical tools such as detonation shock dynamics (DSD) help interpret the effect of various changes to a material on the detonation propagation. Detonation shock velocity (D_n) vs. detonation front curvature (κ) relationships (so-called $D_n - \kappa$ curves) can be generated from the detonation velocity and front curvature measurements during a rate stick experiment. These relationships are important for calibrating shock dynamics models because they are an intrinsic property of the material and thus can be used in configurations other than the measurement geometry.¹¹ However, precise data are needed for DSD calibrations.

Here, we attempt to experimentally isolate the effect of TNT state on Composition B-3 (60% RDX, 40% TNT, no wax) detonation at ambient conditions, at slightly below the melting temperature, and slightly above the melting temperature. This specific formulation is easier to study because there are no additional influences from the wax flowing or melting with temperature. This also means that the molten material is more viscous and so the RDX will take longer to settle or otherwise segregate at temperature. The net effect is advantageous for heating experiments where a single microstructural variable is expected to change (i.e. the TNT melts) and ideally others do not (i.e. RDX movement, TNT bubbling or flowing, etc). The Composition B-3 is machined into pellets, which are assembled into a rate stick and detonated at one end. The detonation velocity is measured with shorting pins and the front curvature of the detonation is measured with a streak camera.

Rate Stick Experimental Setup

Rate sticks are explosive cylinders composed of several cylindrical pellets assembled into a column. Pellets are used for consistency of density throughout the assembly; that is, a single cylinder of pressed or machined HE usually will have

significant density variation between the center of the cylinder and the edges. Generally, the pellets are then bonded together with microns-thick layers of glue and aligned into a single column. Shorting pins are then glued along the cylinder at precise intervals. During the detonation, the shorting pins will short once the insulating material between the two halves of the pin circuit is destroyed by the detonation. This produces a signal which is recorded by an oscilloscope. Precise measurement of the inter-pin spacing and the shorting signal allow for calculation of the detonation velocity. Detonation breakout is measured by using a transparent window with a thin coating of aluminum in a strip of similar width to the charge. The aluminum-coated side is then pressed into intimate contact with the end of the rate stick and held with set screws. An argon flash lamp is triggered to illuminate the aluminum as the detonation progresses through the stick and destroys the aluminum mirror. A streak camera is used to continuously record the reflected light; as the aluminum is destroyed, light is no longer reflected to the camera. Thus a film record of the spatial distribution of the light as a function of time will yield the detonation front shape. This diagnostic is described in more detail elsewhere¹².

For these experiments, Composition B-3 formulated flakes were pressed into cylinders with dimensions of 1-inch-diameter by 2 inches long. The density of the parts was measured and all cylinders fell in the range of 1.7137 – 1.7245 g/cm³. Seven cylinders were used per rate stick. All experiments used a 2-inch-diameter polymethylmethacrylate (PMMA) window with a 6-micron-thick aluminum mirror coated by vapor deposition.

In anticipation of the softening and melting of the TNT in our HE during the elevated temperature experiments, the use of glue or epoxy directly on the surface of the HE was avoided for the entire assembly. Usually, epoxy holds (1) the pellets together, (2) the detonator onto the back of the assembly, (3) the shorting pins in place, and (4) the window on the front of the assembly. Here, detonation in the main charge was initiated by an RP-1 detonator (Teledyne RISI, Tracy, CA, USA), which was held in intimate contact with the Composition B by a spring-loaded sub-assembly. The HE cylinders were encased in a nylon tube (McMaster-Carr, Santa Fe Springs, CA, USA)

with wall thickness of $\frac{1}{4}$ inch. Nylon was chosen for its mechanical stability at elevated temperatures and because it was sufficiently stiff to maintain cylindrical geometry as the Composition B began to soften without being stiff enough to confine the detonation. The nylon tube was machined to provide a moderate slip fit to the Composition B. This allowed the pellets to be secure without requiring glue. The window was held in place with set screws. The entire HE assembly had a slight net compressive stress applied by the spring and detonator in order to keep the HE pellets in contact during the experiment. Holes were drilled in the nylon to allow insertion of thermocouples (Omega, Stamford, CT, USA) in between Composition B pellets and application of shorting pins (Dynasen, Goleta, CA, USA) to the HE surface. Figure 2 shows a schematic and a photograph of one of the rate stick experiments used here.

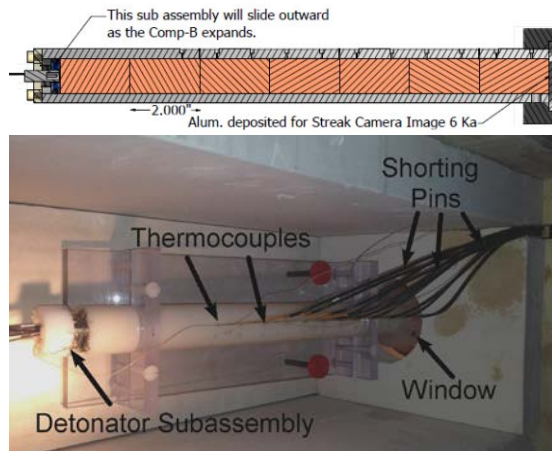


Fig. 2. Composition B-3 rate stick assembly, with schematic (top) and photograph of stick inside a heating apparatus (bottom)

Results and Discussion

Rate Sticks to Examine Temperature Effects

Three rate sticks were assembled and successfully fired: (1) ambient temperature, (2) 70°C , and (3) 85°C . The melting point of TNT is $\sim 80^{\circ}\text{C}$, although our preliminary Composition B research has shown that the bulk formulation does not significantly flow at this temperature. Ideally, these experiments thus capture and differentiate the behavior of Composition B with hot solid TNT from that of Composition B with molten TNT.

Figure 3 shows the shorting pin data for the ambient test, plotting the time the oscilloscope received the signal from each pin (the peaks in the voltage). The spacing between each pin is known, and so the velocity is calculated with a simple linear regression. Figure 4 shows a partial streak camera record from the ambient test.

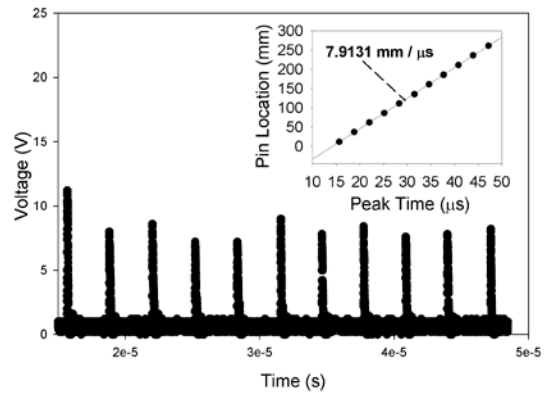


Fig. 3. Shorting pin signals plotted vs. time for the ambient rate stick experiment. Inset is the calculated detonation velocity.

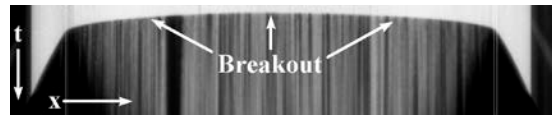


Fig. 4. Streak camera record of detonation breakout for the ambient rate stick experiment (stretched vertically for clarity). The bright region in early time is the intact mirror, so the darkness indicates destruction of the mirror.

The pin data for the ambient test gave a measured detonation velocity of 7.913 ± 0.053 mm / μs . It compares quite well with the available literature. The closest comparable test used Composition B-3 at 2" diameter, with slightly lower density than ours, resulting in less than 1% greater detonation velocity, shown in Table 1.¹²

Elevated temperature tests posed several experimental challenges. The primary concern was the functionality of the RP-1 detonators at temperature. Preliminary heating tests showed that although the internal temperature of the Composition B-3 reached the set point of the box, the exterior of the nylon tube and particularly the detonator (necessarily close to the wall of the box) could reach much higher temperatures. Testing showed that by the time the Composition B-3

reach 90°C, for example, the detonator may have experienced temperatures of 115°C or greater. The PETN in the detonator should decompose around 128°C but certain thermal effects could hinder the ability of the PETN to initiate reliably at temperatures below the decomposition point. However, we wished to continue to use the RP-1 detonator because of its well-characterized and reliable detonation behavior – specifically, the time between sending the electrical signal to explode the bridge wire and the explosive output from the front of the detonator is extremely reliable and repeatable. In order to continue using this detonator at higher temperatures, we made two adjustments to the preliminary setup. First, we custom-built a better heating box with several inches of thermal insulation. Heat was applied from the bottom of the box with a ceramic fiber heating plate (Watlow, St. Louis, MO, USA) rather than through the walls as before. Second, we designed a simple cooling system for the detonator, through which we ran cold tap water. The cooling system is shown on a demo sample of a detonator inside an intentionally-opened nylon tube for illustrative purposes, Figure 5. Detonator cooling tests used several thermocouples to evaluate the efficiency of the cooling system. The details of the test are not particularly interesting but the net result was that the detonator never warmed above 60°C even when the internal box temperature was 115°C, even after soaking at temperature for several hours.

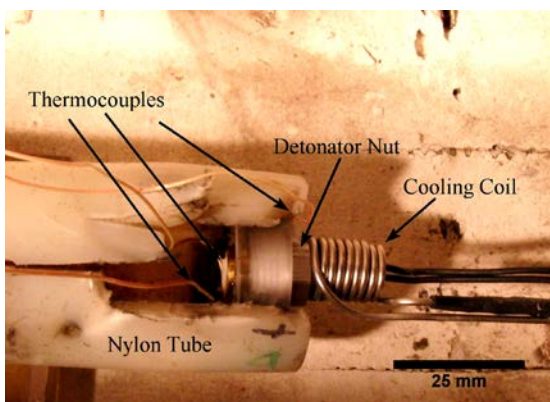


Fig. 5. Setup for cooling experiments using RP-1 detonators. The supply side of the coil was insulated and cold tap water was run through during heating of the box.

Using this modified setup, elevated temperature experiments were conducted at 70°C and 85°C. A summary of the data is given in Table 1. The key finding is that the detonation velocity for the 85°C shot has a value well below that of the 70°C, despite a relatively small increase in temperature, but also a much larger standard error. This indicates that the melting of the TNT affects the detonation propagation significantly.

Table 1. Reported detonation velocity vs. temperature for Composition B-3, with standard error.

Temperature (°C)	Velocity (mm/μs)	Initial Density (g/cm ³)
20	7.913 ± 0.053	1.717 ± 0.003
70	7.884 ± 0.087	1.719 ± 0.001
85	7.808 ± 0.262	1.719 ± 0.002
Ref 2" dia. (ambient) ¹²	7.962	1.707

Detonation Shock Dynamics Calibrations

The film from the streak camera was developed and digitally scanned for the ambient and 85°C shots. Unfortunately, the streak camera image from the 70°C shot was not captured, and we plan to repeat the experiment in the future.

Recall that the streak camera is continuously recording during the experiment, meaning that the resulting film has dimensions of length vs. time. The breakout coordinates can be determined by manually selecting points in the image or by using software routines which attempt to find the edge of an image by using discrete jumps in pixel values. Here, ImageJ (National Institutes of Health) image processing software was used to false-color the grayscale image with a very sensitive color scheme, then to select pixels across the image with the appropriate color. The x-time coordinates of the breakout on the film were converted to x-z coordinates by using the write speed of the camera and the resolution of the scanner. The x-axis is perpendicular to the detonation direction and the z-axis is along it. Figure 6 compares the detonation front curvature of the ambient shot to the 85°C shot. The two-dimensional front curvature measured here can also be considered a cross-section of the three-dimensional front due to the axial symmetry of the rate stick. The x-coordinates

are then simply translated to radial (r) coordinates, facilitating analysis of the relationship between axial and radial propagation.

The data is fit with the function used by Hill et al¹³ which was motivated by Bdzil's earlier work¹⁴

$$z(r) = -\sum_1^n a_n \ln \left[\cos \left(\eta \frac{\pi r}{2R} \right) \right]^n \quad (1)$$

where a_n and η are fitting parameters and R is the measured charge radius.

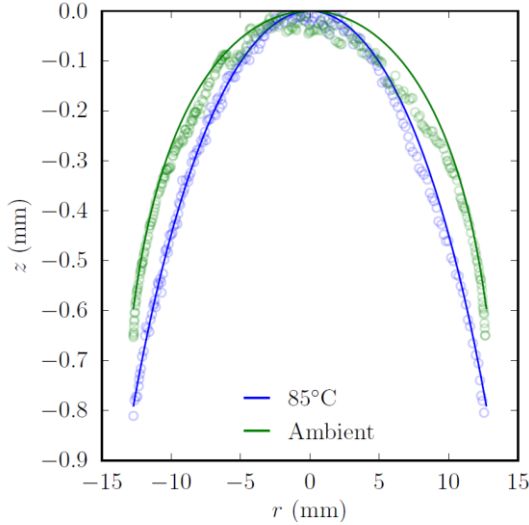


Fig. 6. The detonation front curvature of Composition B-3 at ambient and 85°C. Data is fit with the function proposed by Bdzil.

A few observations on the data are readily apparent. First, the fit to the ambient data is of marginal quality near the core of the sample. The underlying reason for this is currently uncertain. Inspection of Fig. 6 shows a non-symmetric data set about $r=0$. The analytical function is symmetric about $r=0$ and so the marginal quality of fit is due to this variability in the detonation front itself. Material variability is a possible explanation for the non-uniform detonation front. Another explanation could be light transmission issues with the window or film capture with the streak camera. Whatever the reason, this experiment should be repeated to validate the findings. Second, the edge effects of the heated Composition B-3 are much more dramatic than at ambient conditions and the edge angle inferred from the fit is very low for a polymer-confined explosive. The curvature at the front is more significant at 85°C but the curvature near the edges is more significant at ambient.

Once a physical description of the detonation front was obtained, the breakout shape was fitted with Equation 1, with parameters given in Table 2. Also given is the edge angle ϕ , which describes the angle between the detonation front at the edge and the shock wave traveling through the surrounding material (e.g. nylon).

Table 2. Fitting parameters for detonation fronts

Temperature (°C)	a_n	η	ϕ (deg)
20	0.3506	0.8827	11.60
85	1.3260	0.6285	8.87

The normal detonation velocity D_n is a function of the detonation velocity measured by the pins (D_0) and the local angle between the principal axis and the front normal. The curvature κ is a function of the slope of the breakout and the derivative of the slope. The $D_n - r$ curve and $D_n - \kappa$ curve for the ambient temperature Composition B shot is given in Figure 7.

The front curvature calculations reinforce the observations from the raw data, where more of the curvature in the ambient case occurs near the edges while the curvature in the heated case is more balanced but much higher overall. This indicates that the inert confiner is less important to the detonation dynamics at 85°C, and also that the explosive becomes more non-ideal at 85°C.

We note that this is somewhat unanticipated in comparison to the limited data on heated rate sticks in plastic-bonded explosives (PBX). For example, Hill et al studied the effect of temperature on PBX 9502 and found that curvature slightly decreased as temperature increased.¹³ This is generally attributed to a corresponding decrease in the reaction zone size. In that case, the measured detonation velocity did not significantly change with temperature, but the principal difference between any heated PBX experiment and ours is that our matrix material (TNT) is molten at the temperature of interest. The physical state of the TNT would be expected to affect all manner of properties (e.g. modulus, shear strength) and likely correspondingly affects detonation properties. For example, Mader reports the detonation velocity of TNT decreases from 6.950 mm/ μ s to 6.580 mm/ μ s upon melting.⁹ Extension of this type of study to Composition B-3 will be the subject of future investigations.

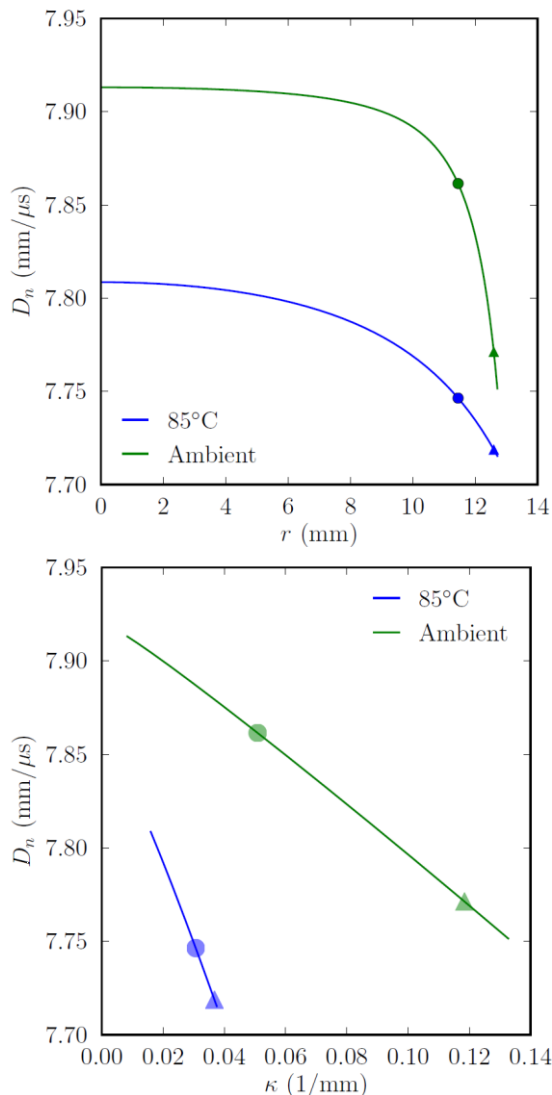


Fig. 7. Detonation velocity as a function of radius (top) and curvature (bottom). Circles indicate 90% of the radius and triangles 99%.

Conclusions

Three rate stick experiments were performed to evaluate the effect of temperature on Composition B-3 detonation dynamics. The results indicate an increasing detonation velocity deficit with temperature. This is consistent with prior work and the expectation that decreasing density due to thermal expansion decreases the energy release. A more significant detonation velocity decrease is associated with the TNT melt in the literature, and we find some evidence for that here.

The associated error of the measurement however is large. The TNT melt certainly appears to significantly shift the $D_n - \kappa$ relationship from the ambient condition.

Due to the large detonation velocity and $D_n - \kappa$ changes observed, additional experimental testing will be required to better understand the relative importance of the thermal expansion and melt phenomena on the detonation dynamics of hot Composition B.

Acknowledgements

The authors wish to thank C. Chiquete (LANL) for some of the DSD analysis and figures. S. Vincent, T. Pierce, T. Tucker, T. Kuiper, and E. Anderson are also thanked for assistance with firing site operations and temperature control of the system.

References

1. Gibbs, T. R., Popolato, A. and Baytos, J. F. "LASL Explosive Property Data" University of California Press, 1980.
2. Gibson, L. L., Dattelbaum, D. M., Bartram, B. D., Sheffield, S. A., Gustavsen, R. L., Brown, G. W., Sandstrom, M. M., Giambra, A. M. and Handley, C. A. "Shock initiation sensitivity and Hugoniot-based equation of state of Composition B obtained using in situ electromagnetic gauging" *Journal of Physics: Conference Series* 500, pp 192004, 2014.
3. Chadd, M. M. and Craig, M. T. "Short pulse duration shock initiation experiments plus ignition and growth modeling on Composition B" *Journal of Physics: Conference Series* 500, pp 052045, 2014.
4. Glascoe, E. A., Hsu, P. C., Keo Springer, H., DeHaven, M. R., Tan, N. and Turner, H. C. "The response of the HMX-based material PBXN-9 to thermal insults: Thermal decomposition kinetics and morphological changes" *Thermochim. Acta* 515, pp 58-66, 2011.
5. Lang, A. J. and Vyazovkin, S. "Ammonium Nitrate-Polymer Glasses: A New Concept for Phase and Thermal Stabilization of Ammonium

Nitrate" *The Journal of Physical Chemistry B* 112, pp 11236-11243, 2008.

6. McKenney, R. L. and Krawietz, T. R. "Binary Phase Diagram Series: HMX/RDX" *Journal of Energetic Materials* 21, pp 141 - 166, 2003.

7. Smilowitz, L., Henson, B., Asay, B. and Dickson, P. "The β - δ phase transition in the energetic nitramine-octahydro-1,3,5,7-tetranitro-1,3,5,7-tetrazocine: Kinetics" *J. Chem. Phys.* 117, pp 3789, 2002.

8. Karpowicz, R. J. and Brill, T. B. "The beta to delta transformation of HMX - Its thermal analysis and relationship to propellants" *AIAA Journal* 20, pp 1586-1591, 1982.

9. Mader, C. L. "Numerical modeling of explosives and propellants." Vol. 1, CRC Press, 1997.

10. Duvall, G. E. and Graham, R. A. "Phase transitions under shock-wave loading" *Reviews of Modern Physics* 49, pp 523-579, 1977.

11. Bdzil, J. B. and Stewart, D. S. "The Dynamics of Detonation in Explosive Systems" *Annual Review of Fluid Mechanics* 39, pp 263-292, 2007.

12. Mader, C. L., Johnson, J. N., and Crane, Sharon L. "Los Alamos Explosives Performance Data" University of California Press, 1982.

13. Hill, L. G., Bdzil, J. B. and Aslam, T. D. "Front curvature rate stick measurements and detonation shock dynamics calibration for PBX 9502 over a wide temperature range" *Proceedings of 11th International Symposium on Detonation*. Medium: ED; Size: 9 p., Snowmass Village, CO.

14. Bdzil, J. B. "Steady-state two-dimensional detonation" *J. Fluid Mech.* 108, pp 195-226, 1981.